Available online at www.sciencedirect.com
ScienceDirect
Journal of Colloid and Interface Science 322 (2008) 136–142
JOURNAL OF Colloid and Interface Science
www.elsevier.com/locate/jcis

Preparation and optical properties of worm-like gold nanorods

Haowen Huang [a,b,*], Chaocai He [a], Yunlong Zeng [a], Xiaodong Xia [a], Xianyong Yu [a,b], Pinggui Yi [a], Zhong Chen [b]

[a] *School of Chemistry and Chemical Engineering, Hunan University of Science and Technology, Xiangtan 411201, PR China*
[b] *State Key Laboratory of Physical Chemistry of Solid Surface, Xiamen University, Xiamen 361005, PR China*

Received 12 October 2007; accepted 1 March 2008

Available online 14 March 2008

Abstract

A type of worm-like nanorods was successfully synthesized through conventional gold nanorods reacting with $Na_2S_2O_3$ or Na_2S. The generated worm-like gold nanorods comprise shrunk nanorod cores and enwrapped shells. Therefore, a gold–gold sulfide core–shell structure is formed in the process, distinguishing from their original counterparts. The formation of the gold chalcogenide layers was confirmed by transmission electron microscopy and X-ray photoelectron spectroscopy. Experimental results showed that the thickness of the gold chalcogenide layers is controllable. Since the increase of shell thickness and decrease of gold nanorod core take place simultaneously, it allows one to tune the plasmon resonance of nanorods. Proper adjustment of reaction time, temperature, additives and other experimental conditions will produce worm-like gold nanorods demonstrating desired longitudinal plasmon wavelength (LPW) with narrow size distributions, only limited by properties of starting original gold nanorods. The approach presented herein is capable of selectively changing LPW of the gold nanorods. Additionally, the formed worm-like nanorods possess higher sensitive property in localized surface plasmon resonance than the original nanorods. Their special properties were characterized by spectroscopic methods such as Vis–NIR, fluorescence and resonance light scattering. These features imply that the gold nanorods have potential applications in biomolecular recognition study and biosensor fabrications.

Keywords: Aspect ratio; Worm-like gold nanorods; Localized surface plasmon resonance; Longitudinal plasmon wavelength

1. Introduction

Gold nanorods exhibit strong optical extinction at visible and near-infrared (NIR) wavelengths where resonant plasmon absorption occurs. This phenomenon is well-suited for photonic, optoelectronic, and biotechnological applications and has thus drawn a lot of attention. Particularly, recent advances in the techniques of synthesis and characterization of plasmon-resonant nanorods are significant, setting the stage for their application toward biomedical imaging and image-guided therapies [1–4].

Gold nanorods demonstrate two plasmon resonance absorption bands: one is around 520 nm, caused by transverse oscillation of electrons, and hence is termed as transverse plasmon wavelength (TPW). The other absorption band in the visible or NIR range is due to the longitudinal oscillation of electrons and is known as longitudinal plasmon wavelength (LPW). Unlike TPW, it depends on the length-to-diameter aspect ratio of the nanorods. As a result, by adjusting the length and diameter of nanorods, the corresponding LPW can be fine-tuned. Several methods have been developed to control the aspect ratio of the gold nanorods [5–8]. Generally speaking, the nanorods having low aspect ratio with longitudinal plasmon band less than 850 nm can be produced readily. For instance, the introduction of silver ion (Ag^+) in growth solution may control the aspect ratio of the gold nanorods [9]. Alternatively, the aspect ratio can be selectively decreased by resizing after growth with other proper additives [10,11]. In comparison, it is challenging to adjust LPW longer than 850 nm of those gold nanorods with high aspect ratio. Current methods are often plagued by poor reproducibility and severe contamination of spherical nanoparticles.

* Corresponding author at: School of Chemistry and Chemical Engineering, Hunan University of Science and Technology, Xiangtan 411201, PR China. Fax: +86 732 8290509.
E-mail address: hhwn@iccas.ac.cn (H. Huang).

0021-9797/$ – see front matter
doi:10.1016/j.jcis.2008.03.004

Therefore, new methodologies that can selectively red shift the LPW of gold nanorods within visible or NIR range are greatly desirable and would significantly augment the study of biosensor and biotechnology.

Here we report a type of gold nanorods. Induced by addition of $Na_2S_2O_3$ to as-synthesized starting solution, the original gold nanorods undergo dramatic increase in width relative to slight change in length. Consequently, worm-like gold nanorods with distinct aspect ratio are formed and exhibit shifted LPW. Even more interesting, the LPW of the nanorods allows selective red-shift through controlling temperature and reaction time. These worm-like gold nanorods are found to be more sensitive to localized surface plasmon resonance (LSPR) absorption than conventional ones, and thus may provide new tools for biosensor and biotechnology research.

2. Materials and methods

2.1. Materials

$HAuCl_4 \cdot 3H_2O$, $AgNO_3$, $NaBH_4$, $Na_2S_2O_3$, cetyltrimethylammonium bromide (CTAB), ascorbic acid were purchased from Sinopharm Chemical Reagent Co., Ltd. (Shanghai, China). Other reagents include *N*-hydroxysuccinimide (NHS) from ACROS (New Jersey, USA), *N*-ethyl-*N*-[(dimethylamino)-propyl]carbodiimide (EDC) from Avocado Research Chemicals Ltd. (Lancashire, UK), mercaptoundecanoic acid (MUA) from Aldrich (Milwaukee, USA) and 3-mercapto-propyl-trimethoxysilane (MPTMS) from Alfa Aesoar (UK). Doubly distilled water was used in all the experiments.

2.2. Preparation of gold nanorods

Gold nanorods were prepared according to previously reported the silver ion-assisted seed-mediated method using CTAB as template [2]. The main steps included making separate seed and growth solution before finally mixing them. Briefly, CTAB solution (1.5 mL, 0.1 M) was mixed with 100 μL of 0.02 M $HAuCl_4$ and stirred. Thereafter, 100 μL ice-cold 0.01 M $NaBH_4$ was added, which resulted in the formation of a brownish yellow seed solution. Vigorous stirring of the solution continued for 2 min before it was kept in a water bath at 25 °C. The seed solution was used at least 2 h after its preparation. To make gold nanorods growth solution, 1.5 mL of 0.02 M $HAuCl_4$ and 1.0 mL of 0.01 M $AgNO_3$ were added into 30 mL of 0.1 M CTAB, and 0.8 mL of 0.08 M ascorbic acid solution was added. Ascorbic acid as a mild reducing agent changes the growth solution from dark yellow to colorless. After both solutions were ready, 70 μL seed was taken out and added to the growth solution at 25 °C. The color of the solution gradually changed in the first 15 min until finally stabilized.

2.3. Preparation of worm-like gold nanorods

50 μL 1 M $Na_2S_2O_3$ solution was added into 3 mL of the as-synthesized gold nanorods at room temperature, heated and kept at 50 °C. Absorption spectroscopy of the resulting nanorods was monitored by a spectrometer of Lambda 35 (Perkin–Elmer). Because the LPW of resulting nanorods red shifted with increasing reaction time, various stages of worm-like gold nanorods were acquired by applying different reaction time intervals, and then the mixture of gold nanorods and $Na_2S_2O_3$ solution was taken out, cooled to room temperature rapidly in ice-water followed by centrifuge and re-dispersion in water solution.

2.4. Immobilization of gold nanorods on glass

Gold nanorods immobilized on glass were used to study their LSPR absorption sensitivity. First, these glass slides (2.2 cm × 1.2 cm) were cleaned by immersion in a piranha solution (consisting of three parts 30% H_2O_2 and seven parts H_2SO_4) at 70 °C for 30 min. After cooling to room temperature, the slides were moved out and rinsed repeatedly with water, and then were sonicated for 10 min. Subsequently, the slides were rinsed repeatedly with ethanol and then immersed in a MPTMS 5% ethanol solution for 4 h. The slides were followed by being rinsed again with ethanol and deionized water in sequence, and air-dried at room temperature prior to further modification. Finally, the mercaptosilane-modified glass slides were incubated in suspension (conventional and worm-like gold nanorods solution, respectively) 30 min to prepare the gold nanorods detection chips. These glass slides immobilized with gold nanorods were measured with a Vis–NIR spectrophotometer.

2.5. X-ray photoelectron spectroscopy

X-ray photoelectron spectra (XPS) were acquired using ESCALab201i-XL spectrometer (VG Scientific Ltd., East Grinstead, Sussex, UK). The base pressure during acquisitions was about 3×10^{-7} Pa. The C1s line (284.6 eV) was used for bending energy calibration.

Throughout the experiments, TEM images of the prepared gold nanorods were taken at 100 kV using Tecnai G2 20AEM (USA). Fluorescence spectra of original gold nanorods and worm-like gold nanorods were obtained using a spectrofluorometer (Hitachi F4500, Japan)

3. Results and discussion

3.1. Key experimental factors for worm-like gold nanorods preparation

The critical role of $Na_2S_2O_3$ for creating the worm-like gold nanorods was evidenced by monitoring real-time extinction spectra during their formation. Fig. 1 shows the temporal evolution of gold nanorods when reacting with $Na_2S_2O_3$ at constant temperature of 50 °C. Initial gold nanorods exhibit one band around 520 nm attributed to TPW, and the other band at a longer wavelength corresponds to LPW. With time increase, a continuous red-shift of LPW accompanied by intensity decrease is observed. Previous reports demonstrate that the LPW of gold

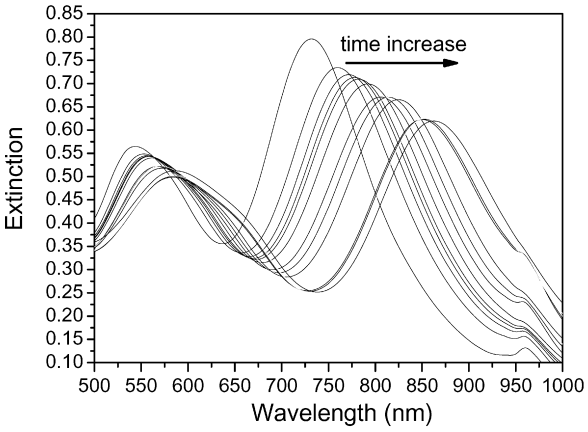

Fig. 1. Extinction spectra of gold nanorods acquired by the as-synthesized gold nanorods reacting with $Na_2S_2O_3$. The solution was a mixture of 3 mL as-synthesized gold nanorods solution and 50 μm 1 M $Na_2S_2O_3$ solution was kept at 50 °C.

nanorods is highly dependent on their length-to-diameter aspect ratio and is influenced drastically even by a slight change [12,13]. In general, LPW shifts to longer wavelength in a linear way when the ratio increases. Hence, the LPW red-shift observed in our experiment should reflect an aspect ratio rise of the generated nanorods. The corresponding TPW on the other hand only displayed minor red-shift from the 520 nm band. In contrast to the characteristic red-brown color of conventional gold nanorods, the formed worm-like gold nanorods solution gradually evolved into deep color until became blue-green with the increase of LPW, as shown in Fig. 2.

The distinct shape and size of worm-like gold nanorods are clearly demonstrated via their TEM images. While conventional gold nanorods (Fig. 3a) overall are rod-like, the worm-like ones (Fig. 3b) produced by addition of $Na_2S_2O_3$ undergo disproportionately larger increase in diameter than in length. As a result, the periphery of these nanorods becomes uniform "loose layer" and serves as a "shell" enwrapping the shrunk original nanorods core. Such a structure looks exactly like a worm, which gives birth to the name of "worm-like nanorods." The size and shape evolution of the worm-like nanorods were monitored by their TEM images, as shown in Fig. 4. The as-synthesized nanorods have an average diameter and length of 12 and 40 nm, respectively (Fig. 4a). During the process of growth, the periphery of gold nanorods becomes loose, particularly in the longitudinal surface. Note that the length does not increase proportionally with the diameter that undergoes significant enlargement. The shell along the longitudinal surface is uniform as shown by TEM images. Fig. 4b displays shells of 2 nm along the longitudinal surface in earlier time, corresponding to a shorter LPW of 817 nm. With time increase, however, the thickness of shells along the longitudinal surface keeps increasing up to 4 nm and 12 nm finally (as shown in Figs. 4c and 4d, corresponding to longer LPW of 823 nm and 978 nm, respectively).

The increase of shell thickness and decrease of gold nanorod core take place simultaneously. As a matter of fact, the shrunk of nanorods core effectively results in their increasing aspect

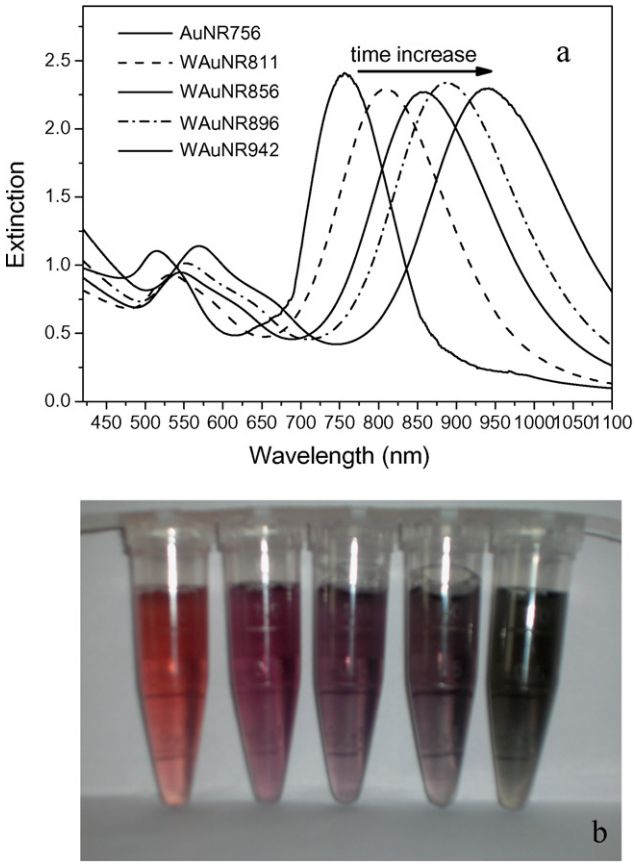

Fig. 2. Optical extinction of gold nanorods and worm-like nanorods with various LPWs at the same concentration, AuNR756 represents gold nanorods possessed LPW 756 and WAuNR811 represents worm-like gold nanorods possessed LPW 811. The bottom digital picture of the products obtained from $Na_2S_2O_3$-induced on gold nanorods, samples from left to right correspond to the curves from AuNR756 to WAuNR942 shown in (a).

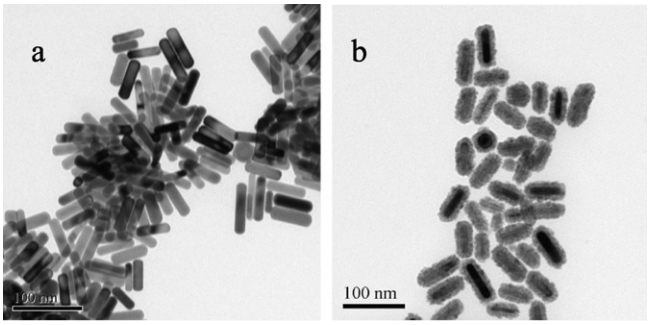

Fig. 3. (a) TEM image of as-synthesized gold nanorods (LPW = 784 nm), and (b) TEM image of formed worm-like nanorods (LPW = 1032 nm) based on the as-synthesized gold nanorods.

ratio, which leads to the observation of considerable red-shift of LPW in extinction spectra. On the other hand, the longitudinal plasmon resonance is attenuated as the thickness of the shell increases. According to previous reports, the phenomenon can be explained as that the enwrapping of the core by the shell screens the incident electromagnetic field [14–16].

Besides the indispensable function of $Na_2S_2O_3$ for synthesis of worm-like nanorods, reaction time is another important factor. As stated above, the increasing thickness of the shell is

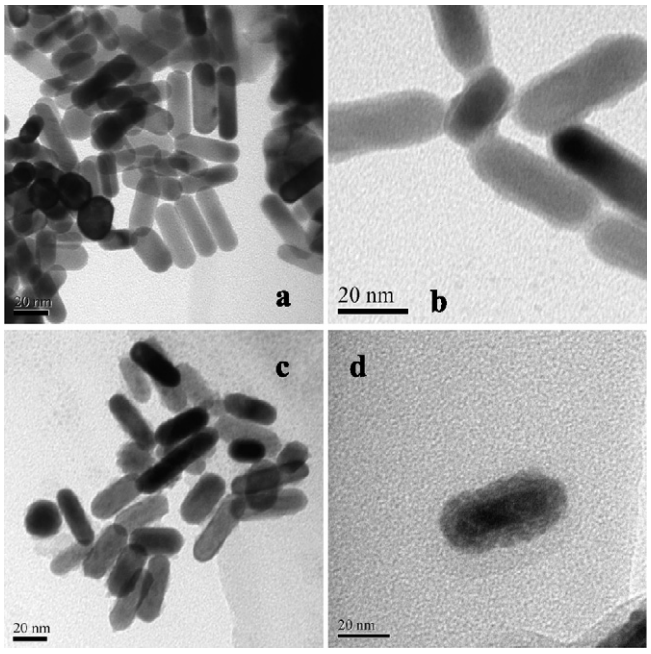

Fig. 4. TEM images elucidate evolution of the worm-like nanorods based on as-synthesized nanorods, (a) represents as-synthesized gold nanorods (LPW = 732 nm), (b) worm-like nanorods with 2 nm shell (LPW = 817 nm), (c) worm-like nanorods with 4 nm shell (LPW = 823 nm), and (d) worm-like nanorods with 12 nm shell LPW = 978.

accompanied by the diminishing of the core during worm-like nanorods formation. Longer reaction time even makes it possible to completely remove the shrunk gold nanorod cores and lead to "worm-like nanorods without cores" as some shown in Fig. 2.

From Figs. 3 and 4, the worm-like nanorods consist of, two distinct phases, cores and shells, which implies the produced shell is distinguished from the original nanorod. As a result of gold nanorods reacting with $Na_2S_2O_3$, we believe the formed shell is another dielectric layer of gold sulfide, and then, enwrapped the decreasing gold nanorod cores in the process of the reaction. This was demonstrated by XPS shown in Fig. 5. During the course of shell growth, the plasmon-related absorption peak undergoes very large shifts in wavelength. This may result from two reasons, one is the coated another dielectric layer may lead to a red shift of plasmon resonance reported by the previous works [17]. Additionally, the aspect ratio of the increasing gold nanorods acted as the core of worm-like nanorods is observed to increase upon growth of the sulfide shell. The final peak position also depends on the aspect ratio of the gold core. This understanding of the optical properties of these nanoparticles is used to elucidate the worm-like nanorods growth kinetics.

There are several other factors crucial to the preparation of worm-like nanorods. First is the involvement of the CTAB.

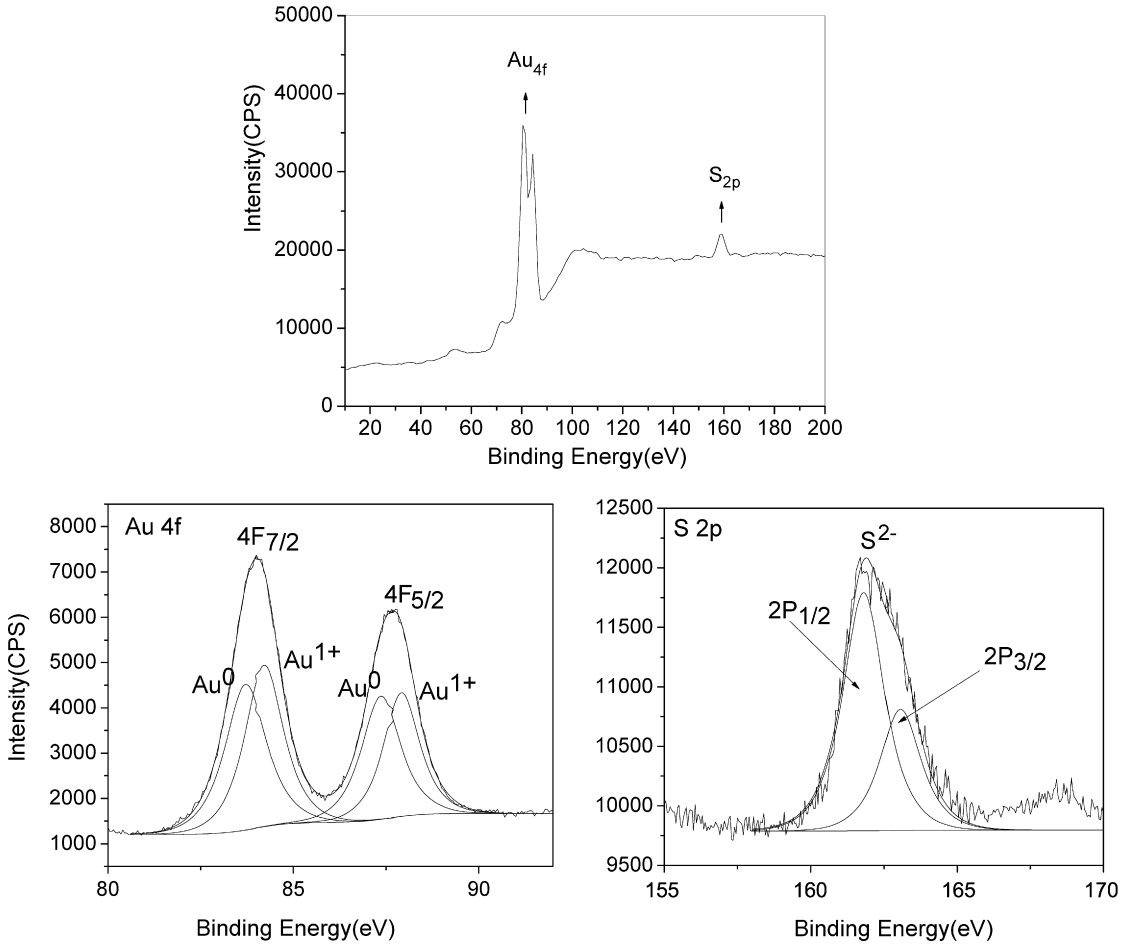

Fig. 5. XPS spectra measured from worm-like gold nanorods, with peak identity labeled by element symbol.

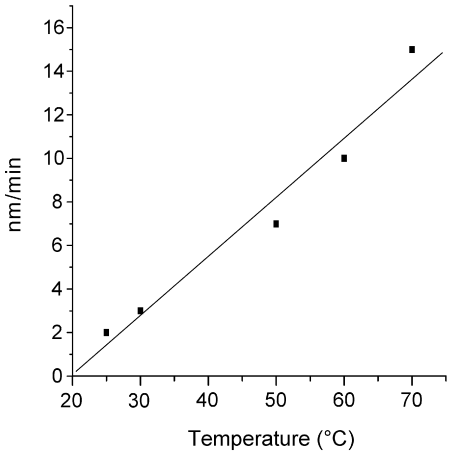

Fig. 6. Relationship between the temperature and the rate of wavelength red-shift.

As discussed above, the as-synthesized nanorods can become worm-like ones with the addition of $Na_2S_2O_3$ in the medium of CTAB solution, and the LPW undergo red shift. However, no red-shift of LPW will be observed if CTAB is removed. Secondly, experiments indicate that the rate of LPW red-shift depended strongly on temperature. At room temperature, $Na_2S_2O_3$ can only induce rather slow red-shift of the nanorods, while raising reaction temperature will significantly accelerate the rate. Fig. 6 shows the relationship between temperature and rate. The red-shift speed almost increases linearly with temperature rise. Thirdly, Na_2S can replace $Na_2S_2O_3$ as the additive to make the worm-like nanorods. Similar red-shift can also be observed when heating the mixture of as-synthesized gold nanorods and Na_2S in CTAB solution. But in comparison with addition of $Na_2S_2O_3$, the shift is much slower. Interestingly, experiments demonstrated the as-synthesized gold nanorods mixed with Na_2S could be stable at room temperature for several months. Hence, Na_2S is often added to serve as stabilizing agent in the gold nanorods solution [18–20].

Combined with various controllable experimental parameters, the worm-like gold nanorods were successfully synthesized by the $Na_2S_2O_3$ dictating method. Some striking properties of the new type of nanorods are noteworthy: the aspect ratio of shrunk gold nanorod cores increase with the increase of thickness of the enwrapped shell; in addition to LPW, their TPW also shows red shift; and interestingly, they disperse in water easier than original nanorods. The dispersion of original gold nanorods is unstable and they quickly precipitate. In comparison, the worm-like gold nanorods can disperse stably for a long period under the same condition, perhaps because the loose structure enlarges the surface of worm-like gold nanorods.

3.2. High sensitivity of worm-like gold nanorods to LSPR absorption

For conventional gold nanorods, the resonance frequency of LSPR is highly sensitive to the dimension, distribution, and shape of the nanostructures as well as to the environment that surrounds them (refractive index of the solvent, binding events, etc.) [21,22]. The same is true for worm-like gold nanorods (see Fig. 1). To further compare the LSPR sensitivity between conventional and worm-like nanorods and investigate their potential for detection chip fabrication, the two types of nanorods were immobilized on separate mercaptosilane-modified glass slides and applied to sense biological binding events. Fig. 7 illustrates their absorption curves in different solvents. More data on the comparison of a series of gold nanorods and worm-like nanorods were listed in Table 1. Based on Fig. 7 and Table 1, it is clear that the worm-like nanorods are more sensitive to the refractive index of the surrounding solvent.

Table 1
Changes of LPW of gold nanorods immobilized on glass slides in different solvents

Solvent	NR[a]	NR[a]	NR[a]	NR[a]	NR[a]	NR[a]	NR[b]	NR[b]
Water	670	700	767	826	847	879	860	879
Chloroform	685	712	790	847	867	912	915	937

[a] Original gold nanorods.
[b] Worm-like gold nanorods.

The glass slides can be further modified with self assembled monolayer (SAM) of MUA. An amine-terminated bovine serum albumin (BSA) was coupled to the carboxylic acid groups of MUA via EDC/NHS activation. Red-shift of 10 and 30 nm was found after the BSA binding on conventional and worm-like gold nanorods, respectively (figures are not shown). The results provide extra evidence that the worm-like gold nanorods show higher sensitivity to LSPR absorption, implying their promising prospects in biomolecular recognition study and biosensor fabrications.

3.3. Other optical properties of worm-like gold nanorods

The worm-like nanorods are also characterized by other optical methods of fluorescence measurement and resonance light scattering (RLS) spectroscopy. Fig. 8a shows the fluorescence spectra of a series of gold nanorods and worm-like nanorods (the same nanorods appeared in Fig. 2) at the same concentration after excitation at 480 nm. As the LPW increases from 756 nm to 942 nm, no significant change of the emission peaks (either the wavelength or the intensity) was observed. The result indicates that the worm-like gold nanorods exhibit similar fluorescence characteristics to the conventional ones.

By setting the detection wavelength equal to the exciting wavelength in fluorescence measurement, RLS spectra are obtained. RLS can provide nanoparticle size and shape information and is thus a very useful tool to study gold nanorods properties. Fig. 8b shows the RLS spectra of the gold nanorods and worm-like nanorods with various LPWs. The gold nanorods display two RLS peaks centered at 340 and 560 nm, attributed to the transverse and longitudinal surface plasmon resonance, respectively. The relative intensity of scattering peaks of nanorods with various LPWs discloses one important observation: the longer LPW the worm-like nanorods have, the higher intensity of their first scattering band and the lower intensity of their second scattering band. To certain extent, the second band

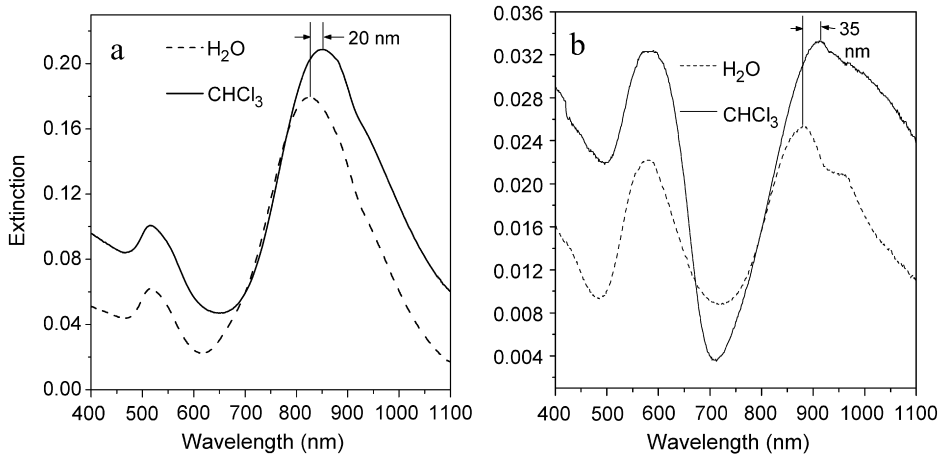

Fig. 7. Extinction spectra of original (a) and worm-like (b) gold nanorods in different solvents. The samples measured are nanorods immobilized on glass slides.

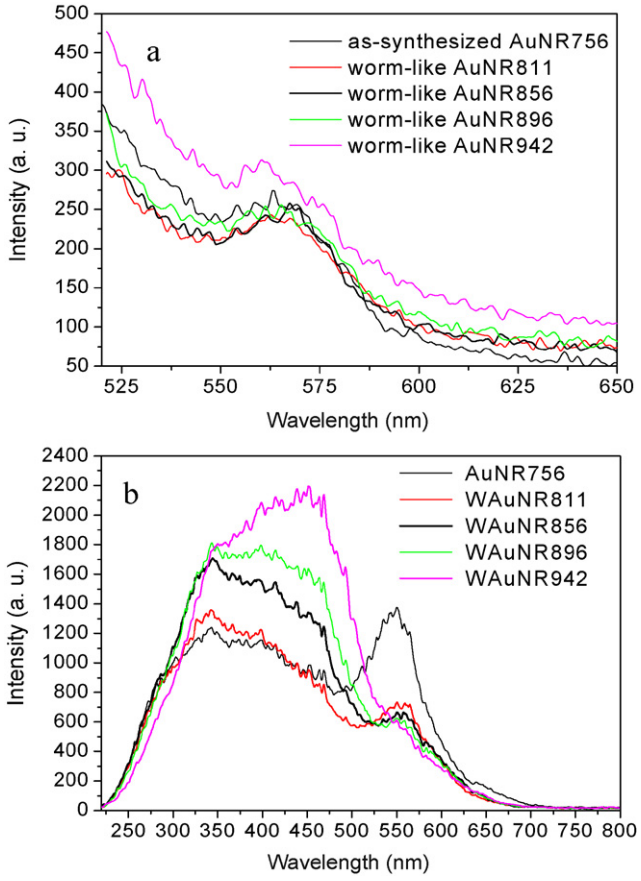

Fig. 8. (a) Fluorescence emission spectra of gold nanorods and the induced worm-like gold nanorods upon 480-nm excitation. (b) Resonance light scattering spectra of gold nanorods shown in Fig. 6a.

will eventually vanishes and only one band is left. It is known that the optical response of gold nanospheres exhibits a single absorption band attributed to the collective dipole oscillation (surface plasmon resonance) [23]. Hence, the RLS characteristics of the worm-like nanorods with 942 nm of LPW turn out to be analogous to those of spheric gold nanoparticles, indicating the influence of shell-wrapped structure on RLS property.

4. Summary

In summary, a type of worm-like gold nanorods was successfully synthesized through the conventional gold nanorods reacting with $Na_2S_2O_3$ or Na_2S. The generated worm-like gold nanorods comprise shrunk nanorod cores and enwrapped shells. Experimental results showed that a gold–gold sulfide core–shell structure is formed in the process, distinguishing from their original counterparts. The formed nanorods have been demonstrated by TEM and XPS. The protocol presented herein opens a new avenue to study biofunctionalization and creation of nanostructured material with controlled dimensions and interactions. Both thickness of shell and size of shrunk gold nanorod cores can be controlled by temperature and reaction time. The feature makes it possible to adjust the aspect ratio of the gold nanorod core and thus allows one to fine-tune the plasmon resonance of created gold nanorods. The worm-like nanorods not only exhibit similar fluorescent and RLS properties of conventional nanorods, but also are more sensitive in LSPR. The features imply that the gold nanorods have potential applications in biosensor fabrication and biotechnology development.

Acknowledgments

This work was supported by Scientific Research Fund of Hunan Provincial Education Department (06B028), Hunan Provincial Natural Science Foundation of China (06JJ30004), Key Project of Health and Science and Technology of Xiamen (3502Z20051027), and National Natural Science Fundation of China (20772027 and 20423002).

References

[1] J. Pérez-Juste, I. Pastoriza-Santos, L.M. Liz-Marzán, P. Mulvaney, Coord. Chem. Rev. 249 (2005) 1870.
[2] A. Brioude, X.C. Jiang, M.P. Pileni, J. Phys. Chem. B 109 (2005) 13138.
[3] K. Sokolov, M. Follen, J. Aaron, I. Pavlova, A. Malpica, R. Lotan, R. Richards-Kortum, Cancer Res. 63 (2003) 1999.
[4] H. Wang, T.B. Huff, D.A. Zweifel, W. He, P.S. Low, A. Wei, J.X. Cheng, Proc. Natl. Acad. Sci. USA 102 (2005) 15752.

[5] B.M.I. van der Zande, M.R. Böhmer, L.G.J. Fokkink, C. Schönenberger, J. Phys. Chem. B 101 (1997) 852.
[6] F. Kim, J.H. Song, P.D. Yang, J. Am. Chem. Soc. 124 (2002) 14316.
[7] B.D. Busbee, S.O. Obare, C.J. Murphy, Adv. Mater. 15 (2003) 414.
[8] H. Huang, C. He, Y. Zeng, X. Xia, X. Yu, Colloids Surf. A 317 (2008) 56–61.
[9] N.R. Jana, L. Gearheart, C.J. Murphy, Adv. Mater. 13 (2001) 1389.
[10] J. Rodríguez-Fernández, J. Pérez-Juste, P. Mulvaney, L.M. Liz-Marzán, J. Phys. Chem. B 109 (2005) 14257.
[11] C.K. Tsung, X.S. Kou, Q.H. Shi, J.P. Zhang, M.H. Yeung, J.F. Wang, G.D. Stucky, J. Am. Chem. Soc. 128 (2006) 5352.
[12] B.H. Yan, Y. Yang, Y.C. Wang, J. Phys. Chem. B 107 (2003) 9159.
[13] X. Kou, S. Zhang, C.K. Tsung, M.H. Yeung, Q. Shi, G.D. Stucky, L. Sun, J. Wang, C. Yan, J. Phys. Chem. B 110 (2006) 16377.
[14] M. Liu, P. Guyot-Sionnest, J. Mater. Chem. 17 (2006) 3942.
[15] I. Pastoriza-Aantos, J. Pérez-Juste, L.M. Liz-Marzán, Chem. Mater. 18 (2006) 2465.
[16] M. Grzelczak, J. Pérez-Juste, F.J.G. de Abajo, L.M. Liz-Marzán, J. Phys. Chem. C 111 (2007) 6183.
[17] R.D. Averitt, D. Sarkar, N.J. Halas, Phys. Rev. Lett. 78 (1997) 4217.
[18] D.A. Zweifel, A. Wei, Chem. Mater. 17 (2005) 4256.
[19] A. Gulati, H. Liao, J.H. Hafner, J. Phys. Chem. B 110 (2006) 22323.
[20] T.B. Huff, M.N. Hansen, Y. Zhao, J.X. Cheng, A. Wei, Langmuir 23 (2007) 1596.
[21] N. Nath, A. Chilkoti, Anal. Chem. 74 (2002) 504.
[22] I. Coille, G. Gauglitz, J. Hoebeke, Anal. Bioanal. Chem. 372 (2002) 293.
[23] Y.Y. Yu, S.S. Chang, C.L. Lee, C.R.C. Wang, J. Phys. Chem. B 101 (1997) 6661.